

# Microwave and Induction Heating-Assisted Biosynthesis of $12\text{CaO}\cdot 7\text{Al}_2\text{O}_3$ Electride from *Aloe Vera* Leaf Extract

Waramon LANGLAR<sup>1\*</sup>, Areeya AEIMBHU<sup>2</sup>, Pichet LIMSUNAN<sup>1</sup>, Chesta RUTTANAPUN<sup>1</sup>

<sup>1</sup> Department of Physics, King Mongkut's Institute of Technology Ladkrabang, Bangkok 10520, Thailand

<sup>2</sup> Department of Physics, Srinakharinwirot University, Bangkok 10110, Thailand

**crossref** <http://dx.doi.org/10.5755/j02.ms.24264>

Received 30 September 2019; accepted 31 December 2019

The white powders used as precursor powders for the synthesis of  $12\text{CaO}\cdot 7\text{Al}_2\text{O}_3$  electride ( $\text{C}_{12}\text{A}_7\text{:e}^-$ ) were prepared by biosynthesis method using *Aloe vera* extract and microwave assisted synthesis. The  $\text{C}_{12}\text{A}_7\text{:e}^-$  crystals were synthesized by induction heating process under a reducing atmosphere at different times of 3, 4 and 5 min. The structure of  $\text{C}_{12}\text{A}_7\text{:e}^-$  powders was characterized by X-ray diffraction. The XRD analysis revealed that pure  $\text{C}_{12}\text{A}_7\text{:e}^-$  powders were obtained from white precursor powders with an induction heating process time of 5 min. To confirm that the white precursor powders were transformed into  $\text{C}_{12}\text{A}_7\text{:e}^-$  after induction heating process for 3, 4 and 5 min, the optical absorption spectra of powders were investigated by an UV-Vis diffuse reflectance spectrometer in the wavelength range of 200–800 nm. The results show the optical absorption bands at 2.8 eV for the white precursor powders with induction heating time of 3, 4 and 5 min. This is due to the  $\text{C}_{12}\text{A}_7$  was transformed into electride ( $\text{C}_{12}\text{A}_7\text{:e}^-$ ). Therefore, the results on the optical absorption spectra are in good agreement with the XRD results.

**Keywords:**  $12\text{CaO}\cdot 7\text{Al}_2\text{O}_3$  electride, *Aloe vera* leaf extract, biosynthesis, microwave assisted, induction heating process.

## 1. INTRODUCTION

Electrides are ionic crystal in which the electrons are trapped in cavities in the host lattice and serve as the counteranions to an equal number of positive charges in regular crystalline array [1]. They are promising materials for various applications such as reducing agents [2–4], cathode materials in electrochemical reaction and fluorescent lamp [5, 6], electron emitters [7–9] and superconductors [10, 11]. Electrides can be classified into 2 types: organic and inorganic electrides.

Organic electrides are crystalline ionic salt in which alkali metal cations ( $\text{Li}^+$ ,  $\text{Na}^+$ ,  $\text{K}^+$ ,  $\text{Rb}^+$  or  $\text{Cs}^+$ ) are complexed by organic molecules such as cryptands and crown ethers that serve to isolate the cations from electrons trapped in cavities or channel [12]. The first organic electride,  $\text{Cs}^+(\text{186C6})_2\text{e}^-$ , was synthesized by Ellaboudy et al. [13] and the crystal structure of  $\text{Cs}^+(\text{186C6})_2\text{e}^-$  was investigated by Dawes et al. [14]. After that, the different organic electrides were synthesized such as  $\text{Cs}^+(\text{186C6})_2\text{e}^-$  [15],  $\text{K}^+(\text{C222})\text{e}^-$  [16, 17],  $\text{L}^+(\text{C211})\text{e}^-$  [18] and  $\text{Rb}^+(\text{C222})\text{e}^-$  [19]. However, the organic electrides were limited by their thermal instability and must be kept at a temperature below  $-40^\circ\text{C}$  [2, 4]. When the organic electrides are exposed to the air and moisture at a temperature above  $-40^\circ\text{C}$ , the decomposition of organic electrides occurred. It is due to the oxygen-carbon bonding in organic molecule is ruptured [1, 20]. Thermal instability are the disadvantage of organic electrides for application in electronic materials. However, the thermal instability at room temperature and above can be improved by replacing oxygen with nitrogen in the complexants [20].

Inorganic electrides are crystalline ionic salts in which the anions are electrons confined in a complex array of cavities or channels and the cations are nanoscale arrays of alkali metal ions that provide charge balance [3, 21]. Inorganic electrides can be prepared by loading alkali metals (Cs, Rb) to the silica zeolites i.e.  $\text{Si}_{32}\text{O}_{64}$  and  $\text{Si}_{64}\text{O}_{128}$  [2, 4], such as Cs-loaded  $\text{Si}_{32}\text{O}_{64}$ . These inorganic electrides are strong reducing agents [2–4].

Matsuishi et al. [22] is the first group to synthesize  $[\text{C}_{24}\text{Al}_{28}\text{O}_{64}]^{4+}\cdot(4\text{e}^-)$  inorganic electride using  $\text{C}_{12}\text{A}_7$  as a precursor. They removed  $\sim 100\%$  of clathrated oxygen ions from the crystallographic cages in a single crystal of  $\text{C}_{12}\text{A}_7$ , leading to the formation of high-density electrons localized in the cages. The  $[\text{C}_{24}\text{Al}_{28}\text{O}_{64}]^{4+}\cdot(4\text{e}^-)$  inorganic electride is regarded as a thermally and chemically stable materials. The  $\text{C}_{12}\text{A}_7$ , an insulating oxide with the chemical formula of  $[\text{C}_{24}\text{Al}_{28}\text{O}_{64}]^{4+}\cdot(2\text{O}^{2-})$  has a unique crystal structure composed of positively charge lattice framework of  $[\text{C}_{24}\text{Al}_{28}\text{O}_{64}]^{4+}$  and 12 subnanometer-sized cages. The cages are three-dimensionally connected and packed by monomolecular oxide layer. Free  $\text{O}^{2-}$  ions are present in 2 out of 12 cages in the unit cell to compensate the positive charge on the cage wall [23]. The insulating oxide  $\text{C}_{12}\text{A}_7$  can be converted into conductor by replacing free  $\text{O}^{2-}$  ions with  $\text{H}^-$  [24] or electron ( $\text{e}^-$ ) [22, 25, 26]. When electrons ( $\text{e}^-$ ) replace free  $\text{O}^{2-}$  ions in  $\text{C}_{12}\text{A}_7$ , it leads to  $\text{C}_{12}\text{A}_7$  electride ( $\text{C}_{12}\text{A}_7\text{:e}^-$ ) with a chemical formula of  $[\text{C}_{24}\text{Al}_{28}\text{O}_{64}]^{4+}\cdot(4\text{e}^-)$ .

In recent years, the ( $\text{C}_{12}\text{A}_7\text{:e}^-$ ) electrides have been synthesized by the treatment of  $\text{C}_{12}\text{A}_7$  with various processes such as: (1) thermal treatment of  $\text{C}_{12}\text{A}_7$  with Ca in vacuum [22]; (2) thermal treatment of  $\text{C}_{12}\text{A}_7$  in Ti metal vapor [25]; (3) thermal treatment of  $\text{C}_{12}\text{A}_7$  under reducing  $\text{CO}/\text{CO}_2$  atmosphere [26]; (4) melt-solidification process of  $\text{C}_{12}\text{A}_7$  under a reducing atmosphere [8]; (5) one-step

\* Corresponding authors. Tel.: +66-89-7623541.

E-mail address: [l.waramon@gmail.com](mailto:l.waramon@gmail.com) (W. Langlar)

thermal treatment of  $\text{Ca}_3\text{Al}_2\text{O}_6$  ( $\text{C}_3\text{A}$ ) +  $\text{CaAl}_2\text{O}_4$  ( $\text{CA}$ ) in graphite reduction [27]. However, these processes require a long treatment time for 2 to 240 h to synthesize  $\text{C}_{12}\text{A}_7\text{:e}^-$ . Recently, Li et al. [7] and Chung et al. [28] using spark plasma sintering (SPS) of  $\text{C}_{12}\text{A}_7$  for the synthesis of  $\text{C}_{12}\text{A}_7\text{:e}^-$ . The  $\text{C}_{12}\text{A}_7\text{:e}^-$  was obtained rapidly within 10–20 min. The *Aloe vera* (*A. vera*) is a perennial, drought-resisting and succulent plant belonging to the Liliaceae family [29]. The *A. vera* leaf consists of three parts: outer layer, middle layer and inner layer. The inner layer composed of large thin walled parenchyma cells that store *A. vera* gel (mucilage) [30]. The *A. vera* gel consists of about 99.5 % water and it has a pH of 4–5 with organic acid, mineral, polysaccharides, vitamin, and protein [29–33]. The *A. vera* gels play a role in synthesizing nanomaterials due to these compounds have the ability to be actively reducing and stabilizing agents responsible for the synthesis of nanostructured materials [34].

Nowadays, the microwave ovens have been widely used in laboratory for materials synthesis due to microwave heating generated internally within the material, instead of originating from the external source [35]. Therefore, it can provide a higher heating rate and a more homogeneous heating [36], leading to a shorter time for the synthesis of precursor materials. Electromagnetic induction heating has been widely used in industry and has been of considerable interest in medical research due to easy to set up, fast-heating, fast-cooling, clean, inexpensive, and energy-saving [37].

In this paper, the rapid synthesis of  $\text{C}_{12}\text{A}_7\text{:e}^-$  crystals by biosynthesis using *A. vera* extract under microwave and induction heating processes is reported. The crystal structure and optical absorption spectra of  $\text{C}_{12}\text{A}_7\text{:e}^-$  were studied. In this work, *A. vera* extract was used to replace chemical acid that generally used in conventional methods for the synthesis of  $\text{C}_{12}\text{A}_7$ . Therefore, the synthesis of  $\text{C}_{12}\text{A}_7\text{:e}^-$  crystals described in this paper is an eco-friendly process [38].

## 2. EXPERIMENTAL DETAILS

### 2.1. Materials

All the chemical materials used for the synthesis of  $\text{C}_{12}\text{A}_7\text{:e}^-$  were analytical grade. Aluminium tri-sec-butoxide ( $\text{Al}[\text{OCH}(\text{CH}_3)\text{C}_2\text{H}_5]_3$ :ATSB) and ethyl aceto- acetate ( $\text{CH}_3\text{COCH}_2\text{COOC}_2\text{H}_5$ :ETAC) purchased from Acros, calcium nitrate tetrahydrate ( $\text{Ca}(\text{NO}_3)_2 \cdot 4\text{H}_2\text{O}$ ) and absolute ethanol purchased from Carlo Ebra.

### 2.2. Preparation of *A. Vera* extract

*A. vera* extract was prepared by removing gel from *A. vera* leaves of about 50 g. It was blended and added with the 100 ml boiled deionized-water. The mixture was heated on the hot plate at 90 °C for 1 h and cooled down to the room temperature. It was filtered and *A. vera* extract solution was obtained. Then, it was stored at a temperature of 4 °C.

### 2.3. Synthesis of $\text{C}_{12}\text{A}_7\text{:e}^-$

The ATSB and  $\text{Ca}(\text{NO}_3)_2 \cdot 4\text{H}_2\text{O}$  were used as starting materials. The ATSB and  $\text{Ca}(\text{NO}_3)_2 \cdot 4\text{H}_2\text{O}$  were mixed

with ETAC by a molar ratio of 12:14:12 and stirred at room temperature for 30 min. Then, the 20.88 ml absolute ethanol was dropped into 37.78 g of the mixture and stirred vigorously at room temperature for 30 min, followed by dropping 25 ml of *A. vera* extract solution and stirred vigorously for 30 min. Finally, the clear and white solution was obtained. The solution was sonicated by an ultrasonic cleaner for 5 h to reduce particle size. The solution was transformed into white colloidal solution. Then, the samples was heated in an electric oven at 90 °C for 18 h and the dry yellow-brown gel was formed. The dry gel was ground and heated in a domestic microwave oven (Samsung, ME711K/XST) for preheating at a power of 800 W for 15 min and preheating at this condition was repeated one more time. After preheating, the white powders were obtained and used as the precursor for the synthesis of  $\text{C}_{12}\text{A}_7\text{:e}^-$ . Three graphite crucibles were prepared and each one was filled with 5 g of precursor powders. All three graphite crucibles were closed with graphite plates. Then, they were placed in the quartz tube and heated in an induction heating oven (CEP, IND4010M) with an applied current in the coil of 4 A and a frequency of 10 kHz as shown in Fig. 1. Three graphite crucibles were heated under the flowing Ar gas for 3, 4 and 5 min, respectively. The temperature at the graphite crucible was measured by a type R thermocouple. Finally, the white powders were melted and transformed into solid and  $\text{C}_{12}\text{A}_7\text{:e}^-$  crystals with dark green color were obtained.

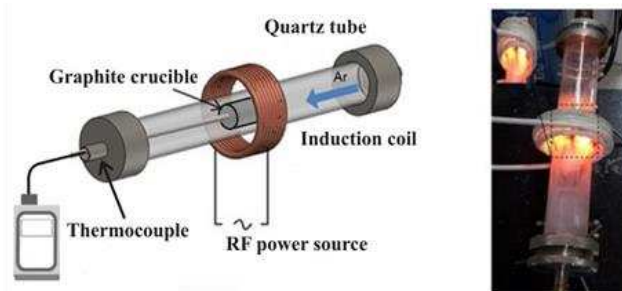


Fig. 1. Induction heating process

### 2.4 Characterization

The  $\text{C}_{12}\text{A}_7\text{:e}^-$  crystal were ground into powders for structure analysis. The structure of  $\text{C}_{12}\text{A}_7\text{:e}^-$  powders was characterized by a X-ray diffractometer (PANalytical, Empyrean) using  $\text{CuK}\alpha$  radiation operated at 40 kV and 40 mA. The XRD patterns were recorded in the  $2\theta$  range of 10° to 80° with a scanning rate of 2°/min. The optical absorption spectra of  $\text{C}_{12}\text{A}_7\text{:e}^-$  powders were determined by an UV-Vis diffuse reflectance spectrometer (Agilent Carry 5000) in the wavelength range of 200–800 nm.

## 3. RESULTS AND DISCUSSION

The XRD patterns of white precursor powders synthesized by microwave-assisted and biosynthesis method are shown in Fig. 2 a and those of  $\text{C}_{12}\text{A}_7$  synthesized via induction heating process for 3, 4 and 5 min are shown in Fig. 2 b. The reference peaks of  $\text{C}_{12}\text{A}_7$  were marked according to JCPDS file number 09-0413. For white powders, the XRD patterns in Fig. 2 a show that the powders consist of  $\text{Al}_2\text{O}_3$ ,  $\text{CaAl}_2\text{O}_4$  ( $\text{CA}$ ),  $\text{Ca}_3\text{Al}_2\text{O}_6$

(C<sub>3</sub>A) and Ca<sub>12</sub>Al<sub>14</sub>O<sub>33</sub> (C<sub>12</sub>A<sub>7</sub>) phase which is not pure C<sub>12</sub>A<sub>7</sub> phase. When the white powders were heated by induction heating process for 3 min, the rapid increase in temperature from the room temperature to 1100 °C and the white color powders was changed to light green color solid (see Fig. 3). The XRD patterns of 3 min induction heating shows the peaks of C<sub>12</sub>A<sub>7</sub> and C<sub>3</sub>A. For 4 min induction heating, the temperature of white color powders was 1159 °C and the white color powders were changed to green color (see Fig. 3). The peaks of C<sub>12</sub>A<sub>7</sub> and small peaks of C<sub>3</sub>A were observed.

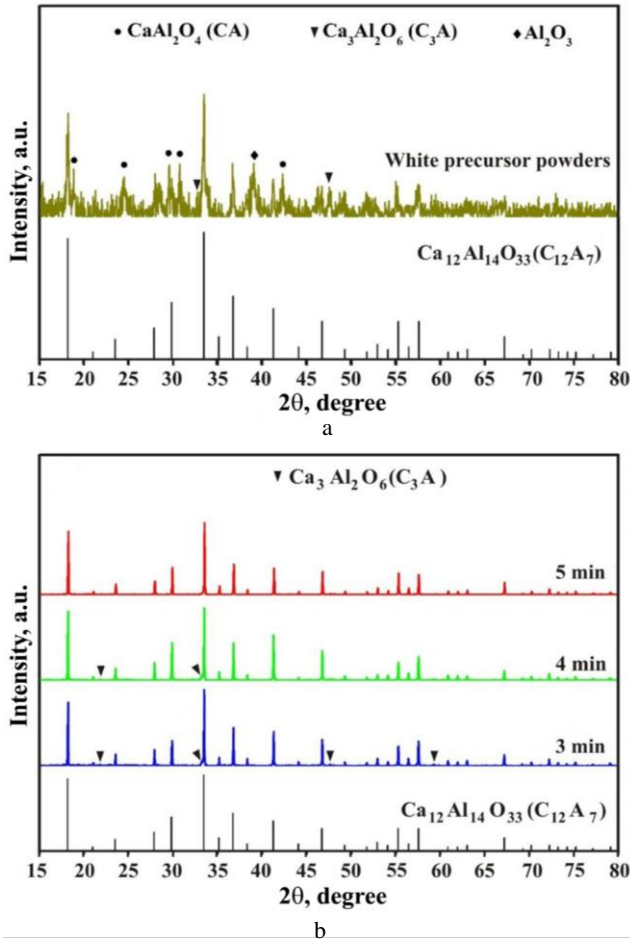


**Fig. 2.** XRD patterns of: a – white precursor powders synthesized by microwave-assisted biosynthesis; b – C<sub>12</sub>A<sub>7</sub> at different induction heating times

For 5 min induction heating, the temperature increased rapidly from room temperature to 1215 °C, the white color powders were changed to dark green color (see Fig. 3). The XRD patterns show only the peaks of pure C<sub>12</sub>A<sub>7</sub> phase.

It is seen that the mixed phase of C<sub>12</sub>A<sub>7</sub> and C<sub>3</sub>A was observed for powders heated with induction heating of 3 and 4 min. However, the pure phase of C<sub>12</sub>A<sub>7</sub> was obtained for powders with induction heating of 5 min. It can be concluded that, for 5 min heating, the temperature reached 1215 °C that close to the melting point of C<sub>12</sub>A<sub>7</sub> (1415 °C) and results in the decomposition of C<sub>3</sub>A to C<sub>12</sub>A<sub>7</sub>. The longer induction heating times from 5 to 7 min were also carried out. It was found that for heating time longer than 5 min such as 6 and 7 min, the powders were not pure

phase of C<sub>12</sub>A<sub>7</sub>. However, the results were not reported here.

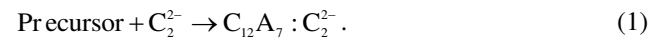
Fig. 3 shows the color of precursor powders and the color of powders after heating at different induction heating times of 3, 4 and 5 min. It is seen that the white precursor powders change to the dark green color of C<sub>12</sub>A<sub>7</sub>:e<sup>-</sup> after heating for 5 min.

To prove that the white precursor powders change to C<sub>12</sub>A<sub>7</sub>:e<sup>-</sup> after induction heating process for 3, 4 and 5 min, the optical absorption spectra of powders were determined by an UV-Vis diffuse reflectance spectrometer in the wavelength range of 200 – 800 nm. Fig. 4 shows the optical absorption spectra obtained from UV-vis diffuse reflectance spectra and converted by Kubelka and Munk theory.

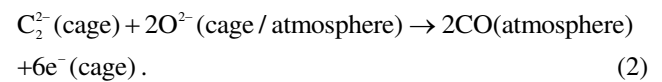
It is seen from Fig. 4 that the white precursor powders have no absorption band at 2.8 eV. However, for all powders heated by induction heating with different times of 3, 4 and 5 min show the absorption band at 2.8 eV. The highest peak of absorption band was observed for powders heated by induction heating for 5 min. It confirms that the white precursor powders completely changed to C<sub>12</sub>A<sub>7</sub> and then transformed to the electride (C<sub>12</sub>A<sub>7</sub>:e<sup>-</sup>). These results are in good agreement with XRD results.

The optical absorption bands at 2.8 eV are responsible for green color to dark green color of C<sub>12</sub>A<sub>7</sub>:e<sup>-</sup>. This is due to the intra-cage transition from the 1s ground state of the occupied cage to 1p excited-state in the same cage [39–41]. The optical transition indicates the electron trapped in the cage of free O<sup>2-</sup> ions. Then, the C<sub>12</sub>A<sub>7</sub> transformed to the electride C<sub>12</sub>A<sub>7</sub>:e<sup>-</sup>.

In the induction heating process, two different ions consist of O<sup>2-</sup> and C<sub>2</sub><sup>2-</sup> ions are important in the synthesis of C<sub>12</sub>A<sub>7</sub>:e<sup>-</sup>. At a high temperature treatment, a strong reducing atmosphere was produced inside the graphite crucible and free O<sup>2-</sup> ion diffuse out of the cage, then the oxygen vacancies were formed at the cage site [26]. Meanwhile, the C<sub>2</sub><sup>2-</sup> ions from graphite crucible were dissolved into the sample molten [8, 39]. Then, the C<sub>2</sub><sup>2-</sup> ions diffuse in the cage of free O<sup>2-</sup> ion to form C<sub>12</sub>A<sub>7</sub>:C<sub>2</sub><sup>2-</sup> molten. When the precursor powders was melted by induction heating process and interacted with graphite crucible, it can be described by reaction:



When the temperature decreased during the cooling process, that is after the induction heating process was turned off, the CO gas evolved. It indicated that C<sub>2</sub><sup>2-</sup> ions were released from the cage of molten and C<sub>12</sub>A<sub>7</sub>:C<sub>2</sub><sup>2-</sup> react with free oxygen ions inside the graphite crucible to form CO gas and generating electron in the cage [8]. The solidification of molten of C<sub>12</sub>A<sub>7</sub>:C<sub>2</sub><sup>2-</sup> transformed to C<sub>12</sub>A<sub>7</sub>:e<sup>-</sup> as follow [8, 39]:





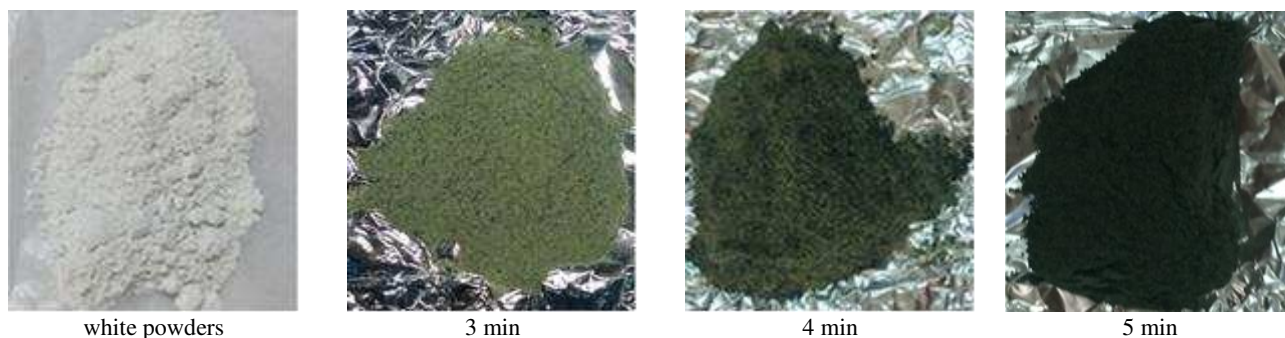


Fig. 3. Color of precursor powders and powders after heating at different induction heating time

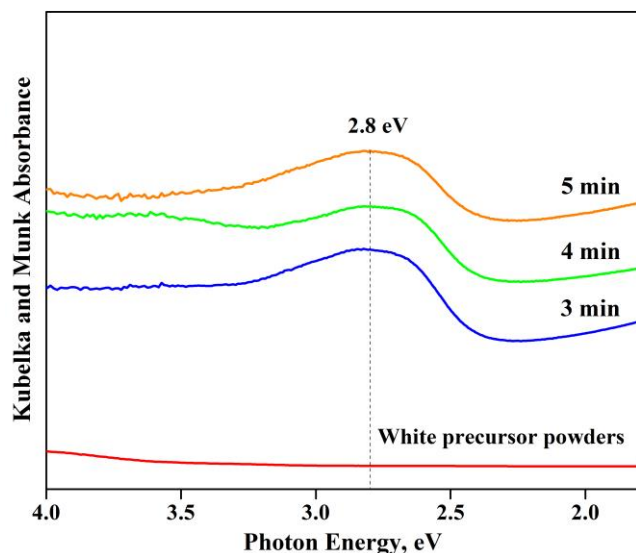


Fig. 4. Optical absorption spectra obtained from UV-vis diffuse reflectance spectra and converted by Kubelka and Munk method of precursor powders and powders after heating at different induction heating times.

#### 4. CONCLUSIONS

We successfully synthesized  $C_{12}A_7:e^-$  crystals rapidly by microwave and induction heating-assisted biosynthesis method using *A. vera* extract. In this work, *A. vera* extract was used to replace chemical acid that generally used in conventional methods for the synthesis of  $C_{12}A_7$ . Therefore, the synthesis of  $C_{12}A_7:e^-$  crystals obtained in this work is an eco-friendly process. The crystal structure and optical absorption spectra of  $C_{12}A_7:e^-$  were studied. The structure of  $C_{12}A_7:e^-$  powders as characterized by X-ray diffraction revealed that pure  $C_{12}A_7:e^-$  crystals were obtained for precursor powders with an induction heating process time of 5 min. The formation of  $C_{12}A_7:e^-$  was confirmed by the optical absorption spectra measurement of powders using an UV-Vis diffuse reflectance spectrometer in the wavelength range of 200–800 nm. The optical absorption bands at 2.8 eV were observed for the white precursor powders after induction heating process for 3, 4 and 5 min. It is due to the  $C_{12}A_7$  was transformed into electride ( $C_{12}A_7:e^-$ ). The results on the optical absorption spectra are in good agreement with the XRD results.

#### Acknowledgments

This work was supported by the Srinakharinwirot University (Grant No. 086/2563).

#### REFERENCES

1. Dye, L.J. Electrides: Early Examples of Quantum Confinement *Accounts of Chemical Research* 42 (10) 2009: pp. 1564–1572. <https://doi.org/10.1021/ar9000857>
2. Ichimura, A.S., Dye, J.L., Camblor, M.A., Villaescusa, L.A. Toward Inorganic Electrides *Journal of the American Chemical Society* 124 (7) 2002: pp. 1170–1171. <https://doi.org/10.1021/ja016554z>
3. Li, Z., Yang, J., Hou, J.G., Zhu, Q. Inorganic Electrides *Chemistry A European Journal* 10 2004: pp. 1592–1596. <https://doi.org/10.1002/chem.200305315>
4. Wernette, D.P., Ichimura, A.S., Urbin, S.A., Dye, J.L. Inorganic Electrides Formed by Alkali Metal Addition to Pure Silica Zeolites *Chemistry of Materials* 15 2003: pp. 1441–1448. <https://doi.org/10.1021/cm020906z>
5. Li, J., Yin, B., Fuchigami, T., Inagi, S., Hosono, H., Ito, S. Application of  $12CaO \cdot 7Al_2O_3$  Electride as a New Electrode for Superoxide Ion Generation and Hydroxylation of an Arylboronic Acid *Electrochemistry Communications* 17 2012: pp. 52–55. <https://doi.org/10.1016/j.elecom.2012.01.024>
6. Watanabe, S., Watanabe, T., Ito, K., Miyakawa, N., Ito, S., Hosono, H., Mikoshiba, S. Secondary Electron Emission and Glow Discharge Properties of  $12CaO \cdot 7Al_2O_3$  Electride for Fluorescent Lamp Applications *Science and technology of advanced materials* 12 (3) 2011: pp. 1–8. <https://doi.org/10.1088/1468-6996/12/3/034410>
7. Li, F., Zhang, X., Liu, H., Zhao, J., Xiao, Y., Feng, Q., Zhang, J. Rapid Synthesis of Inorganic  $[Ca_{24}Al_{28}O_{64}]^{4+}(e^-)_4$  Electride and Its Performance as an Electron Thermal Emitter *Vacuum* 158 2018: pp. 152–157. <https://doi.org/10.1016/j.vacuum.2018.09.055>
8. Kim, S.W., Toda, Y., Hayashi, K., Hirano, M., Hosono, H. Synthesis of a Room Temperature Stable  $12CaO \cdot 7Al_2O_3$  Electride from the Melt and Its Application as an Electron Field Emitter *Chemistry of Materials* 18 (7) 2006: pp. 1938–1944. <https://doi.org/10.1021/cm052367e>
9. Toda, Y., Matsuishi, S., Hayashi, K., Ueda, K., Kamiya, T., Hirano, M., Hosono, H. Field Emission of

- Electron Anions Clathrated in Subnanometer-Sized Cages in  $[\text{Ca}_{24}\text{Al}_{28}\text{O}_{64}]^{4+}(4\text{e}^-)$  *Advanced Materials* 16 (8) 2004: pp. 685–689.  
<https://doi.org/10.1002/adma.200306484>
10. Hosono, H., Kim, S.W., Matsuishi, S., Tanaka, S., Miyake, A., Kagayama, T., Shimizu, K. Superconductivity in Room-Temperature Stable Electride and High-Pressure Phases of Alkali Metals *Philosophical Transactions. Series A, Mathematical, Physical and Engineering Sciences* 373 (2037) 2015: pp. 1–11.  
<https://doi.org/10.1098/rsta.2014.0450>
11. Miyakawa, M., Kim, S.W., Hirano, M., Kohama, Y., Kawaji, H., Atake, T., Ikegami, H., Kono, K., Hosono, H. Superconductivity in an Inorganic Electride  $12\text{CaO}\cdot 7\text{Al}_2\text{O}_3\cdot \text{e}^-$  *Journal of the American Chemical Society* 129 (23) 2007: pp. 7270–7271.  
<https://doi.org/10.1021/ja0724644>
12. Redko, M.Y., Jackson, J.E., Huang, R.H., Dye, J.L. Design and Synthesis of a Thermally Stable Organic Electride *Journal of the American Chemical Society* 127 (35) 2005: pp. 12416–12422.  
<https://doi.org/10.1021/ja053216f>
13. Ellaboudy, A., Dye, J.L., Smith, P.B. Cesium 18-Crown-6 Compounds. A Crystalline Cesium and a Crystalline Electride *Journal of the American Chemical Society* 105 (21) 1983: pp. 6490–6491.  
<https://doi.org/10.1021/ja00359a022>
14. Dawes, S.B., Ward, D.L., Huang, R.H., Dye, J.L. First Electride Crystal Structure *Journal of the American Chemical Society* 108 (12) 1986: pp. 3534–3535.  
<https://doi.org/10.1021/ja00272a073>
15. Dawes, S.B., Eglin, J.L., Moeggenborg, K.J., Kim, J., Dye, J.L.  $\text{Cs}^+(15\text{-Crown-15})_2\text{e}^-$ . A Crystalline Antiferromagnetic Electride *Journal of the American Chemical Society* 113 (5) 1991: pp. 1605–1609.  
<https://doi.org/10.1021/ja00005a025>
16. Huang, R.H., Faber, M.K., Moeggenborg, K.J., Ward, D.L., Dye, J.L. Structure of  $\text{K}^+(\text{cryptand}[2.2.2])$  Electride and Evidence for Trapped Electron Pairs *Nature* 331 1988: pp. 599–601.  
<https://doi.org/10.1038/331599a0>
17. Hendrickson, J.E., Pratt, W.P., Phillips, R.C., Dye, J.L. Optical Spectra and Conductivities of Thin Films of the Electride  $\text{K}^+(\text{cryptand}[2.2.2])\text{e}^-$  *The Journal of Physical Chemistry B* 102 (20) 1998: pp. 3917–3926.  
<https://doi.org/10.1021/jp980564d>
18. Huang, R.H., Wagner, M.J., Gilbert, D.J., Reidy-Cedergren, K.A., Ward, D.L., Faber, M.K., Dye, J.L. Structure and Properties of  $\text{Li}^+(\text{Cryptand}[2.1.1])\text{e}^-$ , an Electride with 1D “Spin-Ladder-like” Cavity-Channel Geometry *Journal of the American Chemical Society* 119 (16) 1997: pp. 3765–3772.  
<https://doi.org/10.1021/ja9640760>
19. Xie, Q., Huang, R.H., Ichimura, A.S., Phillips, R.C., Pratt, W.P., Dye, J.L. Structure and Properties of a New Electride,  $\text{Rb}^+(\text{cryptand}[2.2.2])\text{e}^-$  *Journal of the American Chemical Society* 122 (29) 2000: pp. 6971–6978.  
<https://doi.org/10.1021/ja9943445>
20. Dye, J.L. Electrons as Anions *Science* 301 (5633) 2003: pp. 607–608.  
<https://doi.org/10.1126/science.1088103>
21. Li, Z., Yang, J., Hou, J.G., Zhu, Q. Inorganic Electride: Theoretical Study on Structure and Electronic Properties *Journal of the American Chemical Society* 125 (20) 2003: pp. 6050–6051.  
<https://doi.org/10.1021/ja034020n>
22. Matsuishi, S., Toda, Y., Miyakawa, M., Hayashi, K., Kamiya, T., Hirano, M., Tanaka, I., Hosono, H. High-Density Electron Anions in a Nanoporous Single Crystal:  $[\text{Ca}_{24}\text{Al}_{28}\text{O}_{64}]^{4+}\cdot(4\text{e}^-)$  *Science* 301 (5633) 2003: pp. 626–629.  
<https://doi.org/10.1126/science.1083842>
23. Hosono, H., Hayashi, K., Kamiya, T., Atou, T., Susaki, T. New Functionalities in Abundant Element Oxides: Ubiquitous Element Strategy *Science and technology of advanced materials* 12 (3) 2011: pp. 1–22.  
<https://doi.org/10.1088/1468-6996/12/3/034303>
24. Hayashi, K., Matsuishi, S., Kamiya, T., Hirano, M., Hosono, H. Light-Induced Conversion of an Insulating Refractory Oxide into a Persistent Electronic Conductor *Nature* 419 2002: pp. 462–465.  
<https://doi.org/10.1038/nature01053>
25. Kim, S.W., Matsuishi, S., Nomura, T., Kubota, Y., Takata, M., Hayashi, K., Kamiya, T., Hirano, M., Hosono, H. Metallic State in a Lime-Alumina Compound with Nanoporous Structure *Nano Letters* 7 (5) 2007: pp. 1138–1143.  
<https://doi.org/10.1021/nl062717b>
26. Kim, S.W., Hayashi, K., Hirano, M., Hosono, H., Tanaka, I. Electron Carrier Generation in a Refractory Oxide  $12\text{CaO}\cdot 7\text{Al}_2\text{O}_3$  by Heating in Reducing Atmosphere: Conversion from an Insulator to a Persistent Conductor *Journal of the American Ceramic Society* 89 (10) 2006: pp. 3294–3298.  
<https://doi.org/10.1111/j.1551-2916.2006.01213.x>
27. Jiang, D., Zhao, Z., Mu, S., Phaneuf, V., Tong, J. Simple and Efficient Fabrication of Mayenite Electrides from a Solution-Derived Precursor *Inorganic Chemistry* 56 (19) 2017: pp. 11702–11709.  
<https://doi.org/10.1021/acs.inorgchem.7b01655>
28. Chung, J.H., Ryu, J.H., Eun, J.W., Choi, B.G., Shim, K.B. One-Step Synthesis of a  $12\text{CaO}\cdot 7\text{Al}_2\text{O}_3$  Electride via the Spark Plasma Sintering (SPS) Method *Electrochemical and Solid-State Letters* 14 (12) 2011: pp. E41–E43.  
<https://doi.org/10.1149/2.021112esl>
29. Liu, P., Chen, D., Shi, J. Chemical Constituents, Biological Activity and Agriculture Cultivation of Aloe Vera *Asian Journal of Chemistry* 25 (12) 2013: pp. 6477–6485.  
<https://doi.org/10.14233/ajchem.2013.14418>
30. Boudreau, M.D., Beland, F.A. An Evaluation of the Biological and Toxicological Properties of Aloe Barbadensis (Miller), Aloe Vera *Journal of Environmental Science and Health Part C* 24 (1) 2006: pp. 103–154.  
<https://doi.org/10.1080/10590500600614303>
31. Balaji, A., Vellayappan, M.V., John, A.A., Subramanian, A.P., Jaganathan, S.K., Kumar, M.S., Faudzi, A.A., Supriyanto, M.E., Yusof, M. Biomaterials Based Nano-Applications of Aloe Vera and its Perspective: A Review *RSC Advances* 5 2015: pp. 86199–86213.  
<https://doi.org/10.1039/C5RA13282G>
32. Rahman, S., Carter, P., Bhattarai, N. Review, Aloe Vera for Tissue Engineering Applications *Journal of Functional Biomaterials* 8 (1) 2017: p. 1–17.  
<https://doi.org/10.3390/jfb8010006>

33. **Hamman, J.H.** Review, Composition and Applications of *Aloe vera* Leaf Gel *Molecules* 13 (8) 2008: pp. 1599–1616.  
<https://doi.org/10.3390/molecules13081599>
34. **Dauthal, P., Mukhopadhyay, M.** Nobel Metal Nanoparticles: Plant-Mediated Synthesis, Mechanistic Aspect of Synthesis, and Applications *Industrial & Engineering Chemistry Research* 55 (36) 2016: pp. 9557–9577.  
<https://doi.org/10.1021/acs.iecr.6b00861>
35. **Ramesh, G., Mangalaraja, R.V., Ananthakumar, S., Manohar, P.** Influence of Fuel in the Microwave Assisted Combustion Synthesis of Nano  $\alpha$ -Alumina Powder *International Journal of Physical Sciences* 8 (34) 2013: pp. 1729–1737.  
<https://doi.org/10.5897/IJPS2013.3988>
36. **Boldrini, S., Mortalo, C., Fasolin, S., Agresti, F., Doubova, L., Fabrizio, M., Barison, S.** Influence of Microwave-Assisted Pechini Method on  $\text{La}_{0.80}\text{Sr}_{0.20}\text{Ga}_{0.83}\text{Mg}_{0.17}\text{O}_{3-\delta}$  Ionic Conductivity *Fuel Cells* 12 (1) 2012: pp. 54–60.  
<https://doi.org/10.1002/fuce.201100058>
37. **Wu, C., Li, F., Chen, W., Veeramalai, C.P., Ooi, P.C., Guo, T.** Electromagnetic Induction Heating for Single Crystal Graphene Growth: Morphology Control by Rapid Heating and Quenching *Scientific Reports* 5 (1) 2015: pp. 1–7.  
<https://doi.org/10.1038/srep09034>
38. **Narayanan, K.B., Sakthivel, N.** Green Synthesis of Biogenic Metal Nanoparticles by Terrestrial and Aquatic Phototrophic and Heterotrophic Eukaryotes and Biocompatible Agents *Advances in Colloid and Interface Science* 169 (2) 2011: pp. 59–79.  
<https://doi.org/10.1016/j.cis.2011.08.004>
39. **Kim, S.W., Matsuishi, S., Miyakawa, M., Hayashi, K., Hirano, M., Hosono, H.** Fabrication of Room Temperature-Stable  $12\text{CaO}\cdot 7\text{Al}_2\text{O}_3$  Electride: a Review *Journal of Materials Science: Materials in Electronics* 18 (1) 2007: pp. 5–14.  
<https://doi.org/10.1007/s10854-007-9183-y>
40. **Sushko, P.V., Shluger, A.L., Hayashi, K., Hirano, M., Hosono, H.** Hopping and Optical Absorption of Electrons in Nano-Porous Crystal  $12\text{CaO}\cdot 7\text{Al}_2\text{O}_3$  *Thin Solid Films* 445 (2) 2003: pp. 161–167.  
[https://doi.org/10.1016/S0040-6090\(03\)01156-8](https://doi.org/10.1016/S0040-6090(03)01156-8)
41. **Matsuishi, S., Kim, S.W., Kamiya, T., Hirano, M., Hosono, H.** Localized and Delocalized Electrons in Room-Temperature Stable Electride  $[\text{Ca}_{24}\text{Al}_{28}\text{O}_{64}]^{4+}(\text{O}^{2-})_{2-x}(\text{e}^-)_{2x}$ : Analysis of Optical Reflectance Spectra *The Journal of Physical Chemistry C* 112 (12) 2008: pp. 4753–4760.  
<https://doi.org/10.1021/jp711631j>



© Langlar et al. 2021 Open Access This article is distributed under the terms of the Creative Commons Attribution 4.0 International License (<http://creativecommons.org/licenses/by/4.0/>), which permits unrestricted use, distribution, and reproduction in any medium, provided you give appropriate credit to the original author(s) and the source, provide a link to the Creative Commons license, and indicate if changes were made.